"Colloidal rain" as a novel route to crystallization via viscoelastic phase separation

Hideyo Tsurusawa1, John Russo[1], Mathieu Leocmach[2] and Hajime Tanaka[1,*]

[1]Institute of Industrial Science, University of Tokyo,
4-6-1 Komaba, Meguro-ku, Tokyo 153-8505, Japan

[2]Institut Lumire Matire, CNRS UMR 5306, Universit Claude Bernard Lyon 1,
Universit de Lyon, Lyon, 69622 Villeurbanne Cedex, France

*Corresponding author. E-mail: tanaka@iis.u-tokyo.ac.jp

Received

Here we show by confocal microscopy measurements that crystallization leads to a network structure different from the original phase separation pattern. Crystals nucleate inside the liquid network, and grow past it by direct condensation of the gas phase on their surface, driving evaporation of nearby liquid. This process represents the colloidal analogue of the Bergeron process, i.e., ice crystals formation that occurs in mixed phase clouds and is at the origin of rain. Our *colloidal cold rain* gives us full experimental access to the kinetic pathway of this phenomenon important for climate science. We argue that states similar to colloidal cold rain can form as the result of the gas-liquid phase separation of crystallizable components, such as monoatomic and molecular systems, whose dynamics is slow enough to induce viscoelastic phase separation, but fast enough to prevent immediate vitrification.

Gels and glasses are two important non-ergodic disordered states, which are very important in our life and nature (*4, 5*). The dynamical arrest of colloidal gels and glasses is believed to originate from a dynamical transition to the same non-ergodic disordered glass state, i.e., vitrification. The only difference comes from the fact that the former is formed by densification induced by phase separation and thus is spatially heterogeneous, whereas the latter is formed by uniform densification and is thus spatially homogeneous. Gels are distinct from glasses because of their heterogeneous network structure, which gives them properties intermediate between those of a solid and a fluid phase, and allows the coexistence of two properties usually incompatible with each other, elasticity and fluidity. The elasticity of gels originates from the percolated network structure and the resulting space-spanning connectivity. At the same time a fluid component can easily flow through the elastic network. There are two types of gels with such characteristics: one is a network structure stabilized by stable crosslinks, and the other is a phase-separated structure frozen by dynamical arrest due to vitrification. Many chemical and physical gels belong to the former category, in which the size of network pores is rather small and the fluid transport is not so efficient. On the other hand, gels made of spherical colloids and proteins with attractive interactions belong to the latter category. This type of gels are formed by viscoelastic phase separation (*3, 6*) into a dense liquid phase with slow dynamics and a dilute gas phase with fast dynamics. This difference in the viscoelastic properties between the two phases allows the system to form a space-spanning network structure of the liquid phase, even if it is the minority phase. During phase separation, the density of the liquid phase increases towards the glass-transition density, leading to slow glassy dynamics. At the glass transition point, the percolated network structure is dynamically stabilised by vitrification of the dense liquid phase (*1, 6–13*). More precisely, the dynamical stabilization is due to percolation of locally favored structures, which are

locally stable non-crystalline structures (*14*).

Unlike the above standard scenario of colloidal gelation, it is known that phase separation can also be arrested by crystallization, if the process takes place below the melting point of a component of a mixture (*15*). Indeed the possibility of a different class of gels, which are stabilized by crystallization, was suggested by numerical simulations (*16, 17*) and observed in microgravity experiments (*18*). For colloidal systems, we can in principle access structural evolution in real time at a single-particle level; however, there has so far been no confocal microscopy study on the dynamical process of crystal-gel formation. For confocal microscopy experiments on colloid gelation, colloid-polymer mixtures have so far been used as a model system. The main difficulty consists in the preparation protocol of such a colloid-polymer mixture, where before observation of its dynamics shaking or applying shear is necessary to prepare an initial homogeneous state. This introduces turbulent flows at the beginning of the process, and also does not allow the observation of the initial stages of crystallization. This initial perturbation may even alter the selection of the final non-equilibrium arrested state. In our experiments we instead succeed in building a novel setup that allows the time evolution of the system to be observed directly under the confocal microscope from the very early stages and in a quiescent situation without introducing fluid flows.

In this Letter, we show that, for low polymer concentration, the system can undergo a novel crystallization pathway that leads to the formation of crystalline droplets. These droplets originate from crystal seeds that form inside the liquid branches of the spinodal aggregate, but then grow by direct condensation from the gas phase. The process is analogous to the Bergeron process of ice formation in mixed phase clouds, where ice droplets grow at the expense of the supercooled liquid droplets due to their lower saturated vapor pressure. This is speculated to be the primary mechanism for the formation of

raindrops. In our colloidal system, we then call this process "colloidal cold rain" formation. Due to the difference in the nucleation and growth processes, the droplets display different scaling laws depending on their size. For small nuclei, the droplets have the same fractal dimension of the embedding gel network. But during the growth process, droplets grow with an integer fractal dimension due to direct condensation of gas particles. This is in contrast to the standard crystal-gel scenario, where crystals nucleate and grow inside the dense branches of the gel, becoming dynamically arrested. We also observe that increasing the strength of the interparticle attraction (by increasing the polymer concentration), instead of forming colloidal cold rain, the system undergoes the classical gelation process, in which phase separation is interrupted by vitrification (*1, 6, 9, 19*).

In our experimental setup, the sample cell is put in contact with a reservoir of a salt solution through a semi-permeable membrane (see Methods on the details of our experiments). At $t = 0$, the increase in the concentration of salt ions progressively screens the Coulombic repulsion between colloidal particles, which are then subject to attractive depletion forces, making the system thermodynamically unstable and leading to phase separation. The experimental data is taken at two different volume fractions ($\phi = 0.10$ and $\phi = 0.25$) and for different values of the polymer concentration, $c_p = 0.38, 0.48, 0.57, 1.07$ for $\phi = 0.25$ and $c_p = 0.82, 1.36$ for $\phi = 0.10$. In Fig. 1A, we superimpose the state points with the phase diagram calculated from the YYY equation of state. For each state points, scans at early times (every $10s$) and at the late stage (every $30s$) of the gelation process.

As described above and also in Methods, salt injection initiates liquid-gas phase separation of the colloidal suspension. All samples share the same early stages of spinodal decomposition. Due to strong dynamical asymmetry between colloids and the solvent (*6*), the colloidal particles start aggregating, eventually forming a percolating network. Thus,

a dense network (liquid) coexists with freely diffusing monomers (gas). The topology of the network is similar to all our samples at the initial stages. This is shown for example in Fig. 1B, where we plot the radius of gyration of colloidal clusters (R_g) as a function of the cluster size (s) at the percolation point. Two particles belong to the same cluster if their distance is within the first peak of the radial distribution function. All samples show the same scaling law, which is compatible with the random gelation universality class exponent ($D = 2.53$) as shown by the dashed line in Fig. 1B.

While sharing similar structural properties at early times, the samples differ during the later stages of the phase separation process. To examine this in more detail, we plot in Fig. 1C the structure factor for the final stages of the gelation process for all state points. Calculation of the structure factor is done with the Hanning window function, to minimize boundary effects. The figure shows that at low wavenumber q, the structure factor displays fractal scaling compatible with Guinier law, $S(q) \sim q^{-D}$. But a difference in the fractal dimension D between the $\phi = 0.25$ and $c_p = 0.38$ state point and other state points starts to become visible. In fact, while states with high polymer concentration retain the exponent $D = 2.53$, which is the random gel universality class exponent, as we also observed in the early stages of the gelation process (see Fig. 1B), the state point with low polymer concentration ($\phi = 0.25$ and $c_p = 0.38$) displays the biggest deviation from that exponent. In the figure we also plot the exponent $D = 3$, which corresponds to volume growth, which we will show in the following analysis to be the correct exponent for this state. The difference is due to the onset of crystallization in the low-polymer concentration sample. This is already evident in the high q behavior of the structure factors (Fig. 1C), where the diffraction planes appear as sharper peaks for $\phi = 0.25$ and $c_p = 0.38$.

To gain additional insight, in Fig. 1D we plot the average local volume fraction, com-

puted through Voronoi diagrams, as a function of the number of neighbors. For all state points, we can see that the average volume fraction of a colloidal particle increases with its number of neighbors. Approaching close packing (12 neighbors), we clearly see two family of curves. The state point at $\phi = 0.25$ and $c_p = 0.38$ reaches close packing at a volume fraction of around $\sim 60\%$, which is in reasonable agreement with the volume fraction of the stable crystal phase. All other state points, instead, reach close packing at volume fraction $\sim 55\%$, which is close to the volume fraction of the glass state. This result clearly indicates that the state point at $\phi = 0.25$ and $c_p = 0.38$ follows a different arrest mechanism, in which phase separation is arrested by crystallization and not glassiness. Although our estimation of the absolute volume fraction may involves errors of a few %, the trend should be robust.

To confirm the formation of crystalline seeds we adopt bond orientational analysis to detect which particles are in crystalline environments (*20*). With this analysis we confirm that crystallization events start occurring for the state point $\phi = 0.25$ and $c_p = 0.38$, which has the lowest polymer concentration of all state points. This is shown in Fig. 2A, where the black line indicates the average size of the crystallites, while the red line the average number of crystallites as a function of time. The number of crystallites first rapidly increases as nucleation events start occurring inside the liquid branches, but eventually starts decreasing as the different crystallites grow and merge with each other. All other state points show only negligible signs of crystallization. In particular, for state points with $\phi = 0.25$, increasing polymer concentration drastically reduces the amount of crystals. This is in agreement with the idea of enhanced crystallization rates near metastable critical points (*21, 22*) and the results of Refs. (*16, 17*), which speculated two different arrest mechanisms: crystallization at low polymer concentration, and dynamic arrest at high polymer concentrations.

While nucleation always occurs inside the liquid branches of the phase-separating network, we suggest here the presence of a new growth channel which was neither considered nor observed before. In the following we will show that the growth mechanism of the crystal is not only due to filling of the spinodal liquid network, as was observed in Refs. (*16,17*) for Brownian Dynamics simulations, but also involves direct condensation of the gas phase on the crystalline seeds. To investigate this process, we plot in Fig. 2C the gyration radius of individual crystalline nuclei for the state point $\phi = 0.25$ and $c_p = 0.38$. The results show that the crystal growth follows two different scaling laws: at small crystalline sizes it scales with the dimension of random percolation $D = 2.53$, while at large sizes it scales as $D = 3$ of compact crystal growth. This demonstrates that, while small crystalline nuclei are nucleated inside the phase-separated liquid branches, once they reach the transverse size of the liquid branch, the growth follows a volume expansion with the formation of isotropic droplets (colloidal cold rain). The same scaling law was suggested in the analysis of the structure factors, Fig. 1C, but it is shown directly by the analysis of the gyration radius.

In the next section we demonstrate that the volume growth is due to direct condensation of the gas phase on the crystalline seeds. First we show in Fig. 3A slabs of 10 particle diameter thickness for configurations at $\phi = 0.25$ and $c_p = 0.38$ at different times. Particles are colored according to their phase. The figure shows the first nucleation events inside the liquid network (left panel); then these crystalline nuclei grow directly from the gas phase (middle panel), and finally the different nuclei coalesce (right panel).

Next we show in Fig. 3B the fraction of particles in each different phase for the crystallization trajectory at $\phi = 0.25$ and $c_p = 0.38$, after the liquid-gas phase separation has occurred. The process of crystallization is characterized by a steep decrease in liquid particles, as they transform in small crystalline nuclei inside the liquid domains. This

decrease is accompanied by an increase in the fraction of gas particles: as the first crystals start to appear, liquid particles evaporate to the gas phase due to the higher vapor pressure of the liquid phase compared to the crystalline phase. After the onset of a steady-state gas population, the crystallization proceeds by adding surface particles from the gas phase to the small crystallites. To confirm this process we examine in Fig. 3C the transfer matrix probabilities $P_{\alpha\beta}$, where α and β are each of the phases gas, liquid and crystal (which includes bcc, hcp, fcc and surface particles). Liquid particles undergo two processes, on one hand they transform to crystallites growing inside the liquid branches of the network, and also increasingly transform to gas particles. Gas particles first undergo a transition to liquid particles as the final stage of the liquid-gas phase separation, but once crystalline nuclei outgrow the liquid pockets in which they are formed, the probability for the transition from gas to liquid abruptly decreases. Instead, gas particles start depositing on the crystal, and at later stages the pace of the gas-to-crystal transformation is larger than the one of the liquid-to-crystal one.

We can thus conclude that the crystallization proceeds via two distinct mechanisms: (i) freezing of the fluid; (ii) evaporation of the fluid and condensation of the vapor on the crystals. The first process dominates the initial stages of crystallization, while the second one becomes effective once crystalline nuclei have outgrown the liquid regions in which they form.

The first stages of gelation always involve spinodal decomposition with the formation of a fractal network and gas-liquid phase separation. Depending on the polymer concentration, there are two possible arrest mechanisms. (i) Crystallization, observed at $\phi = 0.25$ and $c_p = 0.38$, small crystalline nuclei appear inside the liquid, reach the surface of the liquid branches, and then grow by addition of particles from the gas phase. The final structure is a network of crystal droplets, as confirmed by the fractal dimension of

the branches, the volume fraction of the particles within the branches, and bond orientational analysis. (ii) Dynamic arrest, particle arrest when the dynamics inside the liquid branch becomes slow, which should happen at the intersection of the glass line with the liquid side of the coexistence curve.

The process we observed is akin to the Bergeron process which is the primary mechanism for the formation of cold rain drops in clouds (*2*). In clouds there is a mixture of ice crystals and supercooled water. The vapor phase is in coexistence with the liquid phase, but is supersaturated with respect to the ice crystals. This causes the water droplets to evaporate and sublimate directly on the ice crystals. Our system can then be regarded as a colloidal analogue for this important process, which can now be studied at the single-particle level.

The basic mechanism creating "crystal gels" may be generic to many other systems. The requirements are (i) the presence of gas-liquid phase separation below the melting point of a crystal, (ii) weak or little frustration against crystallization (in our case, the use of monodisperse colloids), (ii) dynamical slowing down in a supercooled liquid state, which is necessary to induce viscoelastic phase separation leading to the formation of a network structure of the minority phase, and (iii) the degree of supercooling is low enough to avoid a high rate of densification of the liquid phase leading to vitrification. Many monoatomic and single-component molecular systems can satisfy all these conditions in a certain range of the temperature and pressure. This can be seen, for example, by looking at the phase diagram of a Lennard-Jones liquid, which represents many molecular systems without specific directional interactions. Usually, monoatomic systems are very poor glass-formers and thus have not been expected to form gels. However, our mechanism provides a novel kinetic pathway to form network structures made of crystals. So we believe that crystal gels are an important class of heterogeneous non-ergodic states in nature and industrial

applications, although they have not attracted much attention so far.

References

1. P. J. Lu, *et al.*, *Nature* **453**, 499 (2008).

2. T. S. Glickman, W. Zenk, *Glossary of meteorology* (American Meteorological Society, 2000).

3. H. Tanaka, *J. Phys.: Condens. Matter* **12**, R207 (2000).

4. V. J. Anderson, H. N. W. Lekkerkerker, *Nature* **416**, 811 (2002).

5. H. N. W. Lekkerkerker, R. Tuinier, *Colloids and the depletion interaction*, vol. 833 (Springer Science & Business Media, 2011).

6. H. Tanaka, *Phys. Rev. E* **59**, 6842 (1999).

7. P. Pusey, A. Pirie, W. Poon, *Physica A: Statistical Mechanics and its Applications* **201**, 322 (1993).

8. S. M. Ilett, A. Orrock, W. Poon, P. Pusey, *Physical Review E* **51**, 1344 (1995).

9. N. A. M. Verhaegh, D. Asnaghi, H. N. W. Lekkerkerker, M. Giglio, L. Cipelletti, *Physica A: Statistical Mechanics and its Applications* **242**, 104 (1997).

10. G. Foffi, *et al.*, *Phys, Rev. E* **65**, 031407 (2002).

11. E. Zaccarelli, *J. Phys.: Condens. Matter* **19**, 323101 (2007).

12. E. Zaccarelli, P. J. Lu, F. Ciulla, D. A. Weitz, F. Sciortino, *Journal of Physics: Condensed Matter* **20**, 494242 (2008).

13. V. Testard, L. Berthier, W. Kob, *Phys. Rev. Lett.* (2011).

14. C. P. Royall, S. R. Williams, T. Ohtsuka, H. Tanaka, *Nature Mater.* **7**, 556 (2008).

15. H. Tanaka, T. Nishi, *Phys. Rev. Lett.* **55**, 1102 (1985).

16. A. Fortini, E. Sanz, M. Dijkstra, *Physical Review E* **78**, 041402 (2008).

17. T. Pérez, Y. Liu, W. Li, J. Gunton, A. Chakrabarti, *Langmuir* **27**, 11401 (2011).

18. J. Sabin, A. E. Bailey, G. Espinosa, B. J. Frisken, *Phys. Rev. Lett.* **109**, 195701 (2012).

19. C. P. Royall, A. A. Louis, H. Tanaka, *J. Chem. Phys.* **127**, 044507 (2007).

20. J. Russo, H. Tanaka, *Scientific reports* **2** (2012).

21. P. R. ten Wolde, D. Frenkel, *Science* **277**, 1975 (1997).

22. P. D. Olmsted, W. C. Poon, T. McLeish, N. Terrill, A. Ryan, *Physical Review Letters* **81**, 373 (1998).

Acknowledgments H.Ts. and J.R. contributed equally to this work. H.Ta. conceived and supervised the project, H.Ts. performed experiments, J.R. analyzed the data, M.L. calculated the phase diagram, and all the authors discussed and wrote the manuscript. This study was partly supported by Grants-in-Aid for Scientific Research (S) and Specially Promoted Research from JSPS.

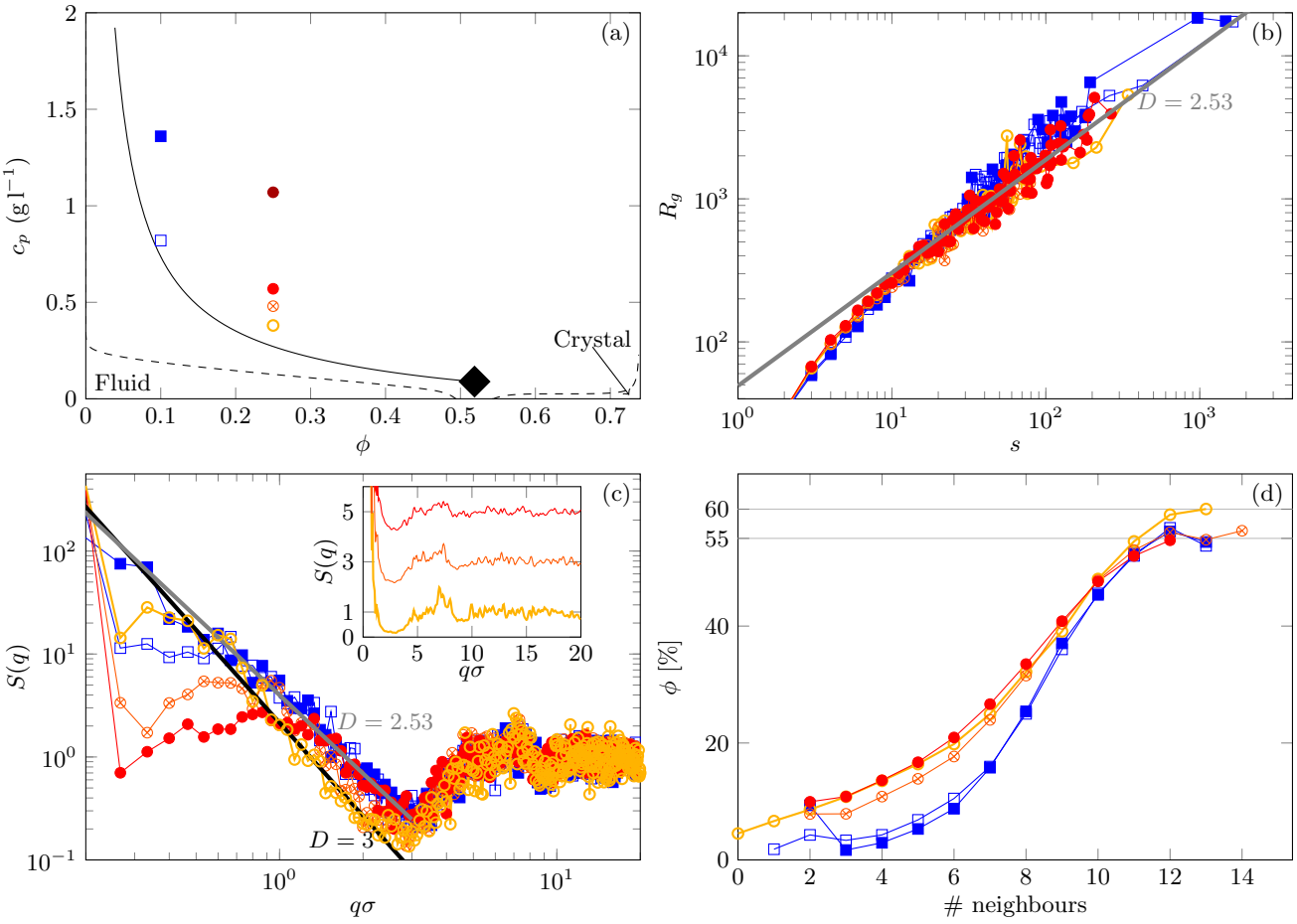

Figure 1: Different routes of viscoelastic phase separation. (A) Phase diagram. Dashed lines are fluid-solid equilibrium coexistence boundaries. The continuous line is the gas side of the metastable gas-liquid spinodal region with the black diamond marking the critical point. The other symbols are the experimental points, consistently used in all panels. (B) Radius of gyration (R_g) as a function of cluster size (s) for all state points at percolation. The gray line represents the fractal dimension of the random gelation universality class. (C) Structure factors for the late stages of the gelation process. The gray and black lines represents respectively random gelation and compact fractal dimensions. (D) Local volume fraction around a colloidal particle, as a function of the number of nearest neighbors of the particle for the state points in the very late stage. Horizontal lines stress the value at 12 neighbors.

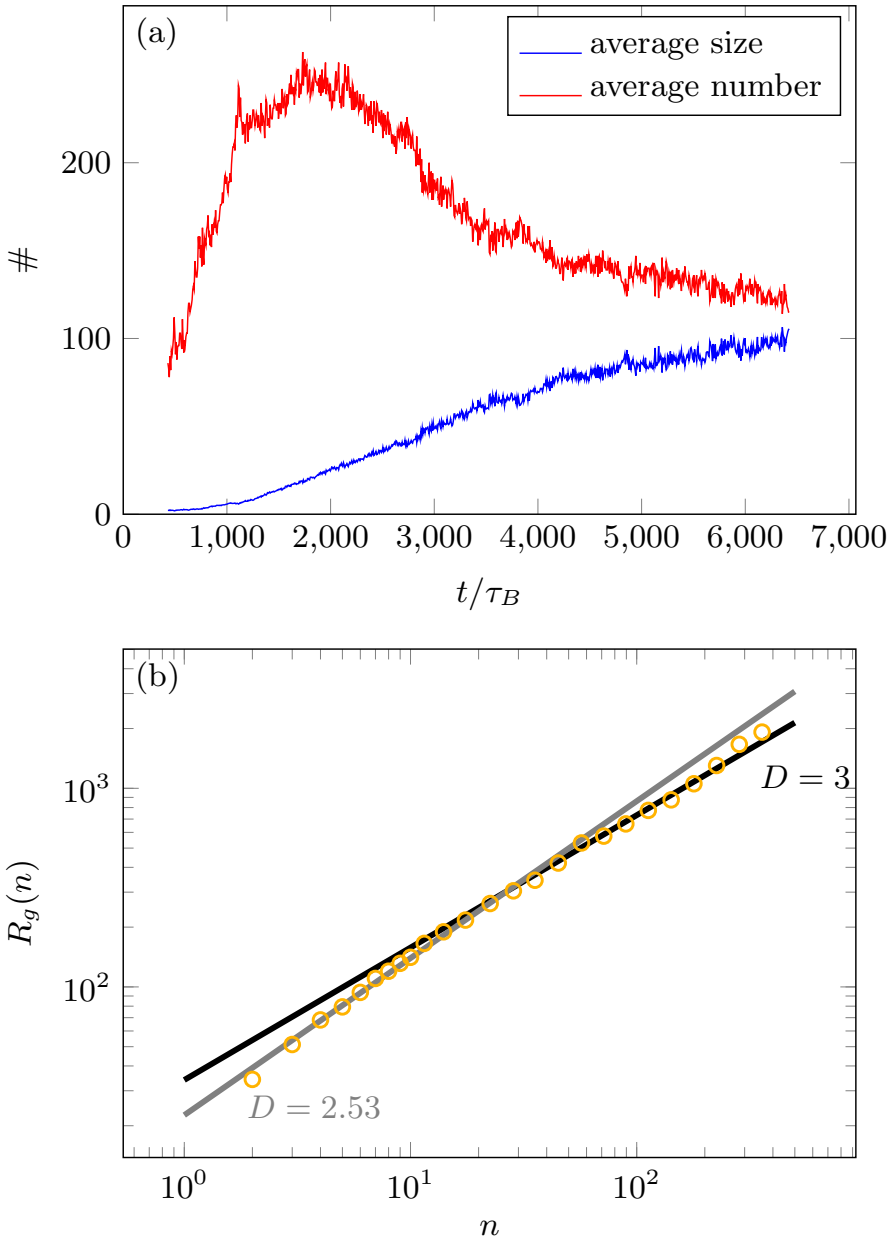

Figure 2: Characterization of the crystal-gel. (A) Time evolution of the average size of the crystals (blue line) and the number of crystals (red line) for the state point $\phi = 0.25$ and $c_p = 0.38$. (B) Radius of gyration of crystalline nuclei at the late stages of gelation for the same state point.

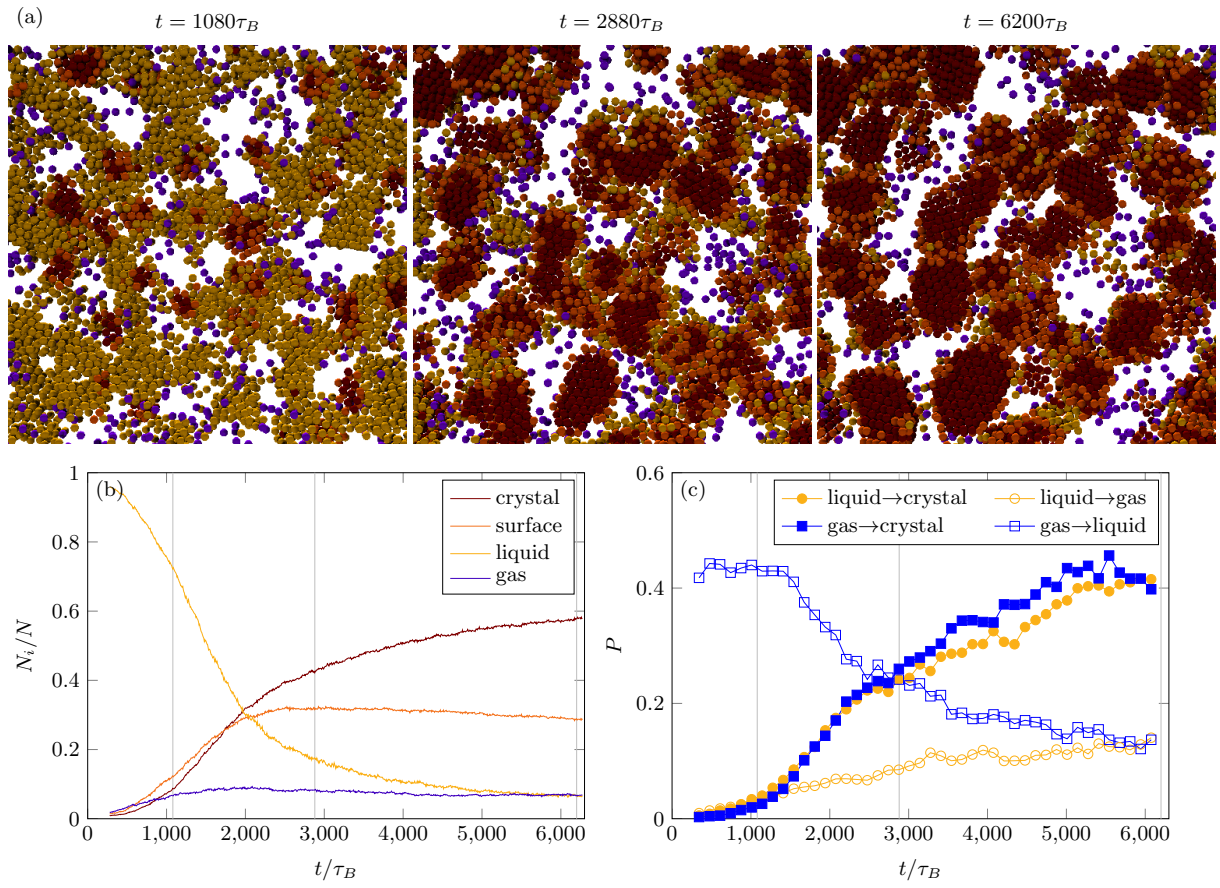

Figure 3: Crystal gel formation. (A) Reconstructions from confocal coordinates at $\phi = 0.25$ and $c_p = 0.38$. Depth of view is 5σ. Particles are drawn to scale and colored according to their phase. Dark red: crystal; orange: surface of crystal; yellow: liquid; blue: gas. (B) Fraction of particles for each phase. Gray vertical lines indicate the times shown in (A). (C) Transition probabilities for the same process as in (B). Here crystal includes surface particles.